

Supporting Information for

Evaluation of the colloidal stability and adsorption performance of reduced graphene oxide–elemental silver/magnetite nanohybrids for selected toxic heavy metals in aqueous solutions

Chang Min Park^{a,b*}, Dengjun Wang^b, Jonghun Han^c, Jiyong Heo^c, Chunming Su^{d, **}

^aDepartment of Environmental Engineering, Kyungpook National University, 80 Daehak-ro, Buk-gu, Daegu, 41566, South Korea

^bNational Research Council Resident Research Associate at the U.S. Environmental Protection Agency, 919 Kerr Research Drive, Ada, OK 74820, USA

*15 ^dGroundwater, Watershed, and Ecosystem Restoration Division, National Risk Management
16 Research Laboratory, Office of Research and Development, U.S. Environmental Protection
17 Agency, 919 Kerr Research Drive, Ada, OK 74820, USA*

*Corresponding author. phone: +82-53-950-6581; fax: +82-53-950-6579;

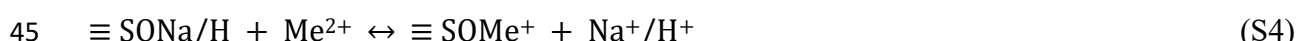
***Corresponding author. phone: +1-580-436-8638; fax: +1-580-436-8703;
e-mail: su.chunming@epa.gov (C. Su)*

23 S1. Adsorption of heavy metal ions by rGO and NHs in single metal system

For single metal system, the adsorption capacities for Cd(II), Ni(II), Zn(II), Co(II), Pb(II), and Cu(II) on rGO, rGO/magnetite, rGO/silver, and rGO/magnetite/silver were compared (Fig. S1). Heavy metal ions were more easily adsorbed on rGO at pH 4 than that of iron- and elemental silver-deposited rGOs (*i.e.*, rGO/magnetite, rGO/silver, and rGO/magnetite/silver), according to following order: Cu(II) > Zn(II) > Ni(II) > Co(II) > Cd(II), Pb(II). The maximum pH at which metallic ions began to hydrolyze was calculated using the solubility product constant (K_{sp}), summarized in Table S1) and metallic ion concentrations to ensure that only dissociated ions would be adsorbed. The K_{sp} value reflects the dissolvability of Me(OH)_2 in water [1], as follows:



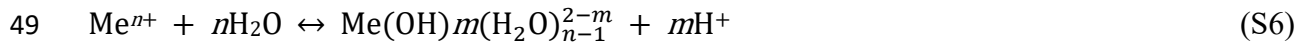
The calculated maximum pH values for Cd(II), Ni(II), Zn(II), Co(II), Pb(II), and Cu(II) were 6.78, 6.87, 6.04, 7.39, 4.58, and 5.10, respectively. At pH levels below these maxima, the adsorption process can be achieved by complex formations with deprotonated sites of the rGO and NHs (Eq. (S3)), exchange with Na^+/H^+ ions (Eqs. (S4) and (S5)), and hydrolysis of metal ions (Me^{2+}) in solution ($n > m$) (Eqs. (S6) and (S7)) [2].



46



48



50



52

53 The physicochemical properties of metallic ions, such as electronegativity, ionic radius, K_{sp} , and
 54 hydrolysis constant (pK_h), are responsible for the adsorption selectivity [3, 4]. The highest
 55 adsorption capacity of Cu(II) on rGO, rGO/magnetite, rGO/silver, and rGO/magnetite/silver
 56 (4.998, 4.203, 4.996, and 4.997 mmol/g, respectively) can be explained by a smallest ionic radius
 57 (0.73 Å) readily occupying the pores of the rGO and NHs despite the low solubility product of
 58 Cu(II) ion (1.6×10^{-19}).

59

60

61 **Table S1.** Hydrolysis constants (pK_h), ionic radii, and solubility products (K_{sp}) of the heavy metal
 62 ions investigated in this study [3, 5, 6].

Heavy metal ions	Cd(II)	Ni(II)	Zn(II)	Co(II)	Pb(II)	Cu(II)
pK_h	10.80	9.40	8.96	9.60	7.71	8.00
Ionic radius (Å)	0.95	0.74	0.75	0.78	1.21	0.73
K_{sp} of $M\text{e(OH)}_x$	7.2×10^{-15}	5.5×10^{-16}	1.2×10^{-17}	5.9×10^{-15}	1.4×10^{-20}	1.6×10^{-19}

63
64

65 **Table S2.** Parameters of the pseudo first-order and second-order kinetic models for Cd(II)
 66 adsorption on rGO, rGO/magnetite, rGO/silver, and rGO/magnetite/silver NHs.

Adsorbent	Exp.	Pseudo-first-order kinetic model			Pseudo-second-order kinetic model		
	$q_{e,exp}$ (mmol/g)	k_1 (1/min)	$q_{e,call}$ (mmol/g)	r^2	k_2 (1/min)	$q_{e,cal2}$ (mmol/g)	r^2
rGO	3.769	0.125	3.835	0.866	0.221	3.811	0.984
rGO/magnetite	2.477	0.070	2.569	0.945	0.171	2.615	0.982
rGO/silver	3.208	0.075	3.322	0.973	0.089	3.427	0.992
rGO/magnetite/silver	3.354	0.101	3.404	0.864	0.209	3.444	0.973

67
68

69 **Table S3.** Parameters of Langmuir and Freundlich isotherms for Cd(II) adsorption on rGO,
70 rGO/magnetite, rGO/silver, and rGO/magnetite/silver NHs.

Adsorbent	Langmuir isotherm model				Freundlich isotherm model			
	$q_e = \frac{q_m b C_e}{1 + b C_e}$	K_L	r^2	χ^2	k_F	n	r^2	χ^2
	(mmol/g)	(L/mmol)						
rGO	3.854	51.90	0.999	1.29×10^{-2}	3.778	12.45	0.910	1.16×10^0
rGO/magnetite	2.605	83.46	0.985	1.14×10^{-1}	2.709	8.850	0.776	4.78×10^{-1}
rGO/silver	3.317	50.25	0.995	8.52×10^{-2}	3.396	7.680	0.854	7.20×10^{-1}
rGO/magnetite/silver	3.441	56.98	0.996	6.10×10^{-2}	3.477	8.718	0.774	7.96×10^{-1}

71
72

73 **Table S4.** Elemental content (%) of the rGO, rGO/magnetite, rGO/silver, and
 74 rGO/magnetite/silver NHs before and after Cd(II) adsorption based on the XPS analyses.

Element	Before Cd(II) adsorption				After Cd(II) adsorption			
	rGO	rGO/ magnetite	rGO/ silver	rGO/ magnetite/ silver	rGO	rGO/ magnetite	rGO/ silver	rGO/ magnetite/ silver
C1s	80.56	42.06	58.42	53.10	77.83	49.74	82.05	30.18
O1s	19.44	52.55	14.91	40.10	20.08	41.17	9.06	54.42
Fe2p3	-	5.38	-	5.23	-	9.03	-	14.44
Ag3d	-	-	26.67	1.56	-	-	8.62	0.59
Cd3d5	-	-	-	-	2.09	0.05	0.27	0.38

75
 76

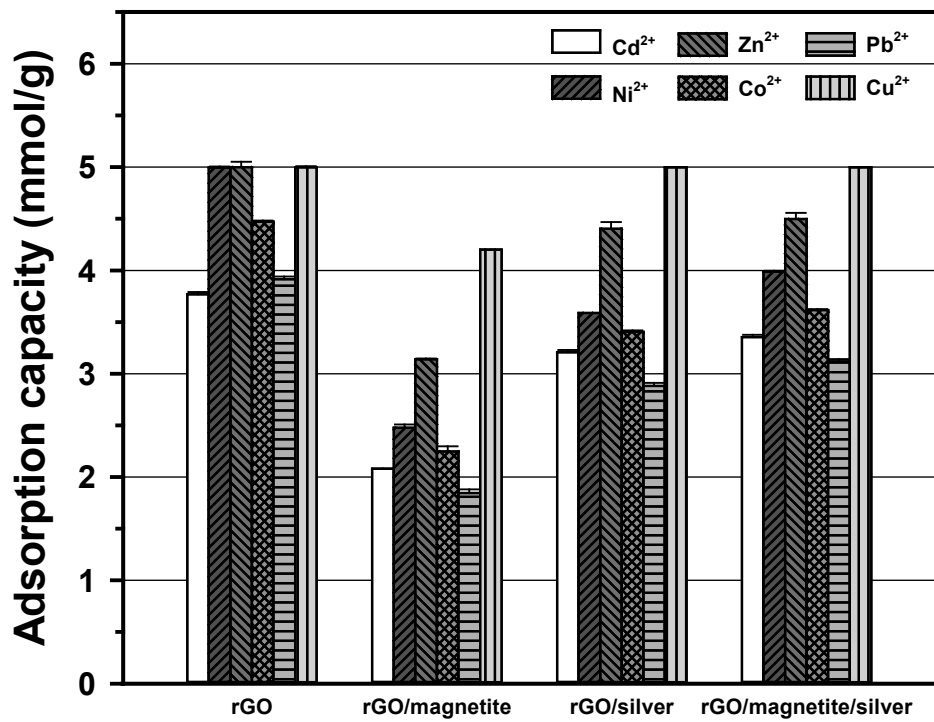
77 **Table S5.** Influence of natural organic matters (Suwannee River humic and fulvic acids) on heavy
 78 metal ion adsorption by rGO, rGO/magnetite, rGO/silver, and rGO/magnetite/silver NHs.

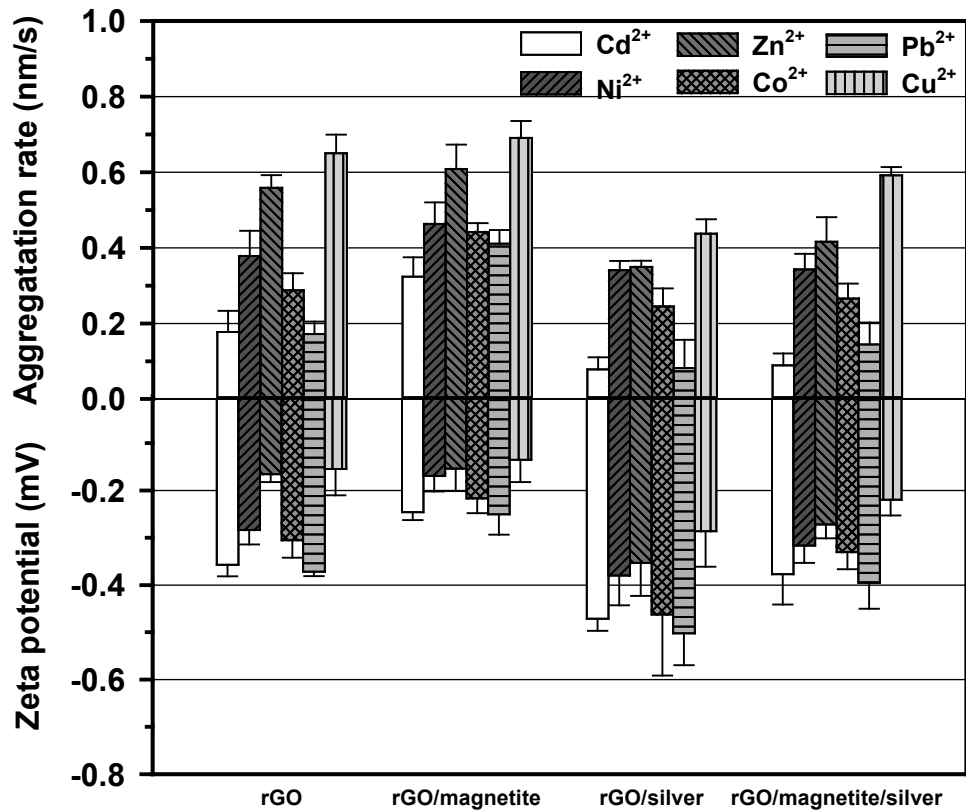
Heavy metals	Adsorbent	Adsorption capacity (mmol/g)		Percentage increase (%)	
		No NOM	Suwannee River humic acid	Suwannee River fulvic acid	Suwannee River humic acid
Cd(II)	rGO	2.55	3.16	3.03	23.79
	rGO/magnetite	1.91	2.85	2.85	48.89
	rGO/silver	2.26	2.86	2.93	26.91
	rGO/magnetite/silver	2.52	2.85	2.91	13.32
Ni(II)	rGO	3.81	3.95	3.74	3.54
	rGO/magnetite	2.32	3.05	3.16	31.58
	rGO/silver	3.18	3.48	3.55	9.45
	rGO/magnetite/silver	3.80	3.84	3.95	1.20
Zn(II)	rGO	5.0	5.0	5.0	0.0
	rGO/magnetite	3.11	3.37	3.48	8.36
	rGO/silver	3.25	3.76	3.74	15.69
	rGO/magnetite/silver	4.15	4.46	4.33	7.47
Co(II)	rGO	2.96	3.86	3.16	30.21
	rGO/magnetite	2.16	2.99	3.08	38.69
	rGO/silver	2.92	2.97	3.21	1.83
	rGO/magnetite/silver	2.95	3.11	3.14	5.47
Pb(II)	rGO	2.76	2.86	3.15	3.81
	rGO/magnetite	1.91	2.88	2.85	51.09
	rGO/silver	2.50	2.19	2.97	-12.29
	rGO/magnetite/silver	2.56	2.66	2.90	3.98
Cu(II)	rGO	5.0	5.0	5.0	0.0
	rGO/magnetite	3.98	4.12	4.18	3.52
	rGO/silver	5.0	5.0	5.0	0.0
	rGO/magnetite/silver	5.0	5.0	5.0	0.0

79

80

81 **Fig. S1.** Comparison of the adsorption capacity of Cd(II), Ni(II), Zn(II), Co(II), Pb(II), and Cu(II)
 82 by rGO, rGO/magnetite, rGO/silver, and rGO/magnetite/silver nanohybrids. Experimental
 83 conditions: $m/V = 0.2 \text{ g/L}$; initial pH = 4.0 ± 0.1 ; $[\text{Cd(II)}]_0 = [\text{Ni(II)}]_0 = [\text{Zn(II)}]_0 = [\text{Co(II)}]_0 =$
 84 $[\text{Pb(II)}]_0 = [\text{Cu(II)}]_0 = 1 \text{ mM}$; $I = 0.01 \text{ mol/L NaNO}_3$; and $T = 298 \text{ K}$.
 85

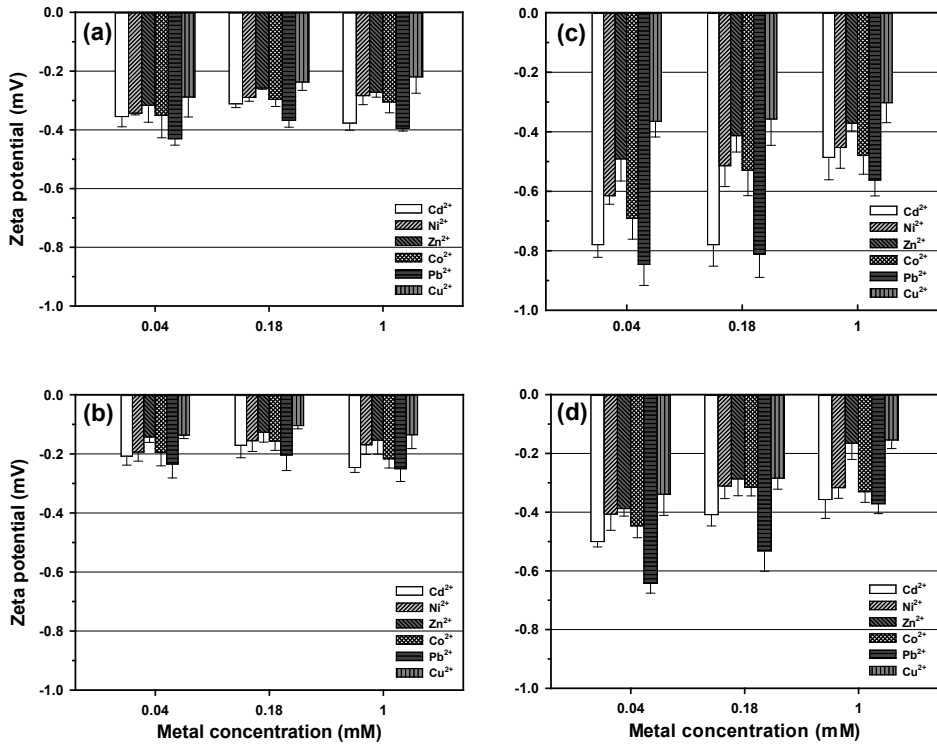




86

87 **Fig. S2.** Aggregation rate plots and zeta potentials of rGO, rGO/magnetite, rGO/silver, and
88 rGO/magnetite/silver nanohybrids with heavy metal ions. Experimental conditions: $m/V = 0.2 \text{ g/L}$;
89 $[\text{Cd(II)}]_0 = [\text{Ni(II)}]_0 = [\text{Zn(II)}]_0 = [\text{Co(II)}]_0 = [\text{Pb(II)}]_0 = [\text{Cu(II)}]_0 = 1 \text{ mM}$; and $T = 298 \text{ K}$.

90



91

92 **Fig. S3.** Comparison of the zeta potential of (a) rGO, (b) rGO/magnetite, (c) rGO/silver, and
 93 (d) rGO/magnetite/silver nanohybrids with heavy metal ions. Experimental conditions: $m/V = 0.2 \text{ g/L}$;
 94 $[\text{Cd(II)}]_0 = [\text{Ni(II)}]_0 = [\text{Zn(II)}]_0 = [\text{Co(II)}]_0 = [\text{Pb(II)}]_0 = [\text{Cu(II)}]_0 = 0.04, 0.18, \text{ and } 1 \text{ mM}$; and $T =$
 95 298 K.
 96

97 **References**

- 98 [1] J.C. Rivière, S. Myhra, Handbook of surface and interface analysis: methods for problem-
99 solving, CRC press, 2009.
- 100 [2] S. Yang, J. Hu, C. Chen, D. Shao, X. Wang, Mutual effects of Pb(II) and humic acid adsorption
101 on multiwalled carbon nanotubes/polyacrylamide composites from aqueous solutions, Environ.
102 Sci. Technol., 45 (2011) 3621-3627.
- 103 [3] Ö. Yavuz, Y. Altunkaynak, F. Güzel, Removal of copper, nickel, cobalt and manganese from
104 aqueous solution by kaolinite, Water Res., 37 (2003) 948-952.
- 105 [4] A. Jang, Y. Seo, P.L. Bishop, The removal of heavy metals in urban runoff by sorption on
106 mulch, Environ. Pollut., 133 (2005) 117-127.
- 107 [5] D. Yu, W. Jillek, E. Schmitt, Electrochemical migration of Sn-Pb and lead free solder alloys
108 under distilled water, J. Mater. Sci. - Mater. Electron., 17 (2006) 219-227.
- 109 [6] D.R. Lide, CRC handbook of chemistry and physics, CRC Press/Taylor and Francis, Boca
110 Raton, FL, 2012.
- 111
- 112